Preparation of polydimethylaminoethyl methacrylate grafted attapulgite via ceric ion-induced redox polymerization

Hang Xu,[1] Haicun Yang,[3] Sheng Xue,[1] Ji Pan,[1] Qingting Ni,[1] Fanghong Gong[1,2]

[1]College of Materials Science and Engineering, Changzhou University, Changzhou 213164, China
[2]School of Mechanical Technology, Wuxi Institute of Technology, Wuxi 214121, China
[3]Institute of Functional Polymers, School of Materials Science and Engineering, Tongji University Shanghai 201804, China
Correspondence to: F. Gong (E-mail: fhgong@cczu.edu.cn)

ABSTRACT: Hybrid nanocomposites consisting of polydimethylaminoethyl methacrylate (PDMAEMA) and attapulgite (ATP) were prepared by using a surface thiol-Ce (IV) redox initiation system via graft from approach. Initially, ATP was chemically modified with γ-mercaptopropyltrimethoxysilane (MTS) to anchor thiol groups on the surface (ATP-MTS). Subsequently, surface-initiated polymerization of dimethylaminoethyl methacrylate was performed by using ATP-MTS and cerium (IV) ammonium nitrate (CAN) in aqueous nitric acid (HNO_3) to afford hybrid particles (ATP-g-PDMAEMA). Evidence of grafting of PDMAEMA was confirmed by Fourier transform infrared spectroscopy (FTIR), X-ray photoelectron spectroscopy (XPS), and Thermogravimetric Analysis (TGA). The crystal structure of PDMAEMA grafted ATP was characterized by X-ray diffraction (XRD) analysis. Morphology of ATP-g-PDMAEMA was observed by transmission electron microscopy (TEM). The effects of concentration of Ce (IV), HNO_3, and reaction temperature were examined by determining the percentage of grafting (PG). With other condition kept constant, the optimum conditions were obtained as follows: the reaction temperature was 50°C, Ce (IV) and HNO_3 concentrations were 12.5 mmol/L and 1 mol/L, respectively, when 0.2 g of ATP-MTS, 1 mL of DMAEMA, and 4 mL of aqueous solution were used. © 2015 Wiley Periodicals, Inc. J. Appl. Polym. Sci. **2015**, *132*, 42762.

INTRODUCTION

Exploiting the fascinating properties of inorganic particles such as optical, magnetic, and electronic properties requires a homogeneous dispersion of particles.[1–3] Grafting polymers on the surface covalently is the best way to avoid aggregation.[4,5] Generally, polymer chains can be introduced on the surface of inorganic particles by "grafting to" and "grafting from" methods. For "grafting to," the reaction between the functionalized macromolecules and particles is hindered sterically.[6,7] On the other hand, "grafting from" method is carried out through the surface anchoring of initiating groups and the subsequent in situ initiated polymerization. Grafting polymer chains are formed through the diffusion of low molecular weight monomer instead of macromolecules in "grafting to" method.[8,9]

Modification of inorganic particles with grafting polymers has attracted considerable interests.[10–12] Surface-initiated graft polymerizations of various monomers onto inorganic nanoparticles have been reported by using UV-induced polymerization,[13] conventional radical polymerizations,[14] and controlled/living radical polymerizations (CRPs).[15,16] CRPs have advantages of the controllable architecture, molecular weight, and molecular weight distribution in comparison with conventional free radical polymerization. However, the condition of most CRPs on the surface of nanoparticles is usually stringent and complicated to operate.

Except for anchoring conventional initiating groups, for example, peroxy and azo groups,[17–19] a redox initiation consisting of the electron donor and accepter is a very efficient method of generating free radicals under mild conditions.[20] Conventional redox initiation pairs include aliphatic amine-persulfate, aromatic tertiary amine-peroxide, and reducing groups-high oxidation state metal ions have been greatly applied for initiating graft polymerization reactions.[21–23] Different from the other dual active sites, redox initiation system with metal ions owns a single active site, which can enhance the graft efficiency effectively. Due to the large reduction potential value, low toxicity, experimental simplicity, and solubility in a number of organic solvents, cerium (IV) has recently emerged as a versatile reagent for oxidative electron transfer.[24,25] Redox initiation systems can

be made up of cerium (IV) and various reducing agents, such as hydroxyl, amines, amides, hydroxycarboxylic acid, and thiols in the aqueous polymerization.[26–30] Thiols are also usually used in the synthesis of branched polymer and the molecular weight regulation.[31,32]

Attapulgite (ATP) is a type of crystalline hydrated magnesium aluminum silicate with exchangeable cations in its framework channels and reactive hydroxyl groups on the surface. ATP has the structural formula of $Si_8O_{20}Mg_5(Al)(OH)_2(H_2O)_4 \cdot 4H_2O$, which was early illustrated in 1940 by Bradley and later further refined.[33,34] The higher aspect ratio, excellent mechanical strength, and thermal stability endow ATP a wide application in the adsorbent,[35] catalyst,[36] especially the reinforcing filler in nanocomposites.[37] However, the aggregation problem of ATP has not been resolved effectively until now.

Recently, we have reported the results of our research on the surface modification of ATP by graft polymerization via aliphatic amine-ammonium persulfate, aromatic tertiary amine-benzoyl peroxide redox system, and thiol-caprolactam two-component iniferter system.[38–40] In this work, ATP was firstly modified to bear thiol groups, and then polydimethylaminoethyl methacrylate (PDMAEMA) was grafted from the surface of ATP by using a thiol-Ce (IV) initiation system. The resulting grafted particles were characterized using Fourier transform infrared (FTIR) spectroscopy, X-ray photoelectron spectroscopy (XPS), X-ray diffraction (XRD), thermogravimetric analysis (TGA), and Transmission electron microscopy (TEM) methods. The polymerization kinetics and the effect of polymerization conditions on the percentage of grafting (PG) were investigated systematically.

EXPERIMENTAL

Materials

Attapulgite (ATP) was supplied by Jiangsu NDZ Technology (Jiangsu, China). It was activated with hydrochloric acid of 1 mol/L for 24 h, and centrifuged, dried in a vacuum at 120°C for 36 h before use. γ-mercaptopropyltrimethoxysilane (MTS, 95%) was purchased from Aladdin-reagent (Shanghai, China). N,N-dimethylaminoethyl methacrylate (DMAEMA) was purchased from Aladdin-reagent (Shanghai, China). It was distilled under reduced pressure. Stock solution of Ce (IV) was prepared from cerium (IV) ammonium nitrate (CAN) in aqueous nitric acid (HNO_3). CAN was supplied by Aladdin-reagent (Shanghai, China) and used as received. All organic solvents were of analytical grade and used as received.

Surface Modification of ATP with MTS

For ATP surface functionalization, 1 g ATP particles was dispersed in 150 mL dimethylbenzene in a 250 mL round bottom flask, and the mixture was stirred with the aid of ultrasonic wave for 30 min. About 2 mL MTS was added dropwise within 30 min and then the reaction mixture was maintained at reflux for 24 h with a strong mechanical stirring in a pure nitrogen atmosphere. The thiol-functionalized particles ATP-MTS were isolated by an ultracentrifuge, washed several times with ethanol to remove the dimethylbenzene and unreacted MTS, and dried in vacuum at 50°C for 24 h.

Preparation of ATP-g-PDMAEMA via Thiol-Ce (IV) Redox Initiation System

A typical procedure for preparation of ATP-g-PDMAEMA hybrids was as follows: 1 g DMAEMA, 0.2 g ATP-MTS, and a teflon-coated stir bar were placed in a 25 mL Schlenk tube. An appropriate amount of CAN in aqueous HNO_3 was then added dropwise to the solution in the tube with continuous stirring. The mixture was ultrasonicated for 30 min to obtain a stable dispersion. The solution was purged with nitrogen and heated to 55°C. Polymerization was maintained for 8 h. After polymerization, the solution was cooled to room temperature and the crude products were centrifuged and dispersed with dimethyl sulfoxide (DMSO) for several times to remove the free polymer. The final product ATP-g-PDMAEMA was dried in a vacuum oven at 50°C for 24 h.

Characterization

Fourier transform infrared spectrum was collected by an Avatar 370 FTIR spectrometer (FTIR, Nicolet) in the frequency range between 4000–500 cm^{-1}. Each spectrum was an average of 16 scans recorded by using a transmission mode at a resolution level of 2 cm^{-1}. X-ray Photoelectron Spectroscopy data was obtained from an Escalab 250Xi spectrometer (XPS, Thermo Fisher) in an ultra-high vacuum using Al K_α radiation at high voltage of 1360 eV. Gaussian-Lorentzian functions were used to perform the curve fitting of the high-resolution spectrum. X-ray Diffraction experiment was carried out on a 18 kw rotating anode X-ray generator (XRD, Rigaku, Japan) with Cu K_α ($\lambda = 1.5406$ Å) radiation operated at 40 kV and 100 mA within the 2θ range of 3° to 60° at a scanning rate of 1°/min. Thermogravimetric Analysis was conducted by using a TG209 F3 system (Netzsch, Germany) at a heating rate of 10°C/min under continuous nitrogen flow. A sample weight of about 3 mg was used for all the measurements and scanned within the temperature range 50–850°C. Transmission electron microscopy (TEM, JEM-1200 EX/S, Japan) was carried out with an accelerating voltage of 200 kV. The dried particles were ultrasonicated in tetrahydrofuran (THF) for 30 min and then deposited on a copper grid covered with a perforated carbon film. The percentage of grafting (PG) and grafting efficiency (GE) were calculated according to the following equations.[40]

$$\text{Percentage of grafting (PG)} = w_2 - w_1 \tag{1}$$

$$\text{Grafting efficiency (GE)} = \frac{m_1 \times \frac{PG}{1-PG}}{m_2 \times C} \times 100\% \tag{2}$$

where w_1 and w_2 (%) are the total weight loss of ATP-MTS and ATP-g-PDMAEMA, respectively; m_1 and m_2 (g) is the weight of ATP-MTS (0.2 g) and monomer (1.0 g), respectively; and C (%) is the monomer conversion.

RESULTS AND DISCUSSION

The graft polymerization of DMAEMA on the surface of ATP is shown in Scheme 1. Thiol groups were introduced to the surface of ATP through surface dealcoholization reaction of ATP and MTS. Ce (IV) ions coupled with thiols on the surface of ATP, which formed thiol-Ce (IV) complex. Subsequently, surface carbon free radicals were generated via single electron transfer-based oxidation processes of complex, and these free
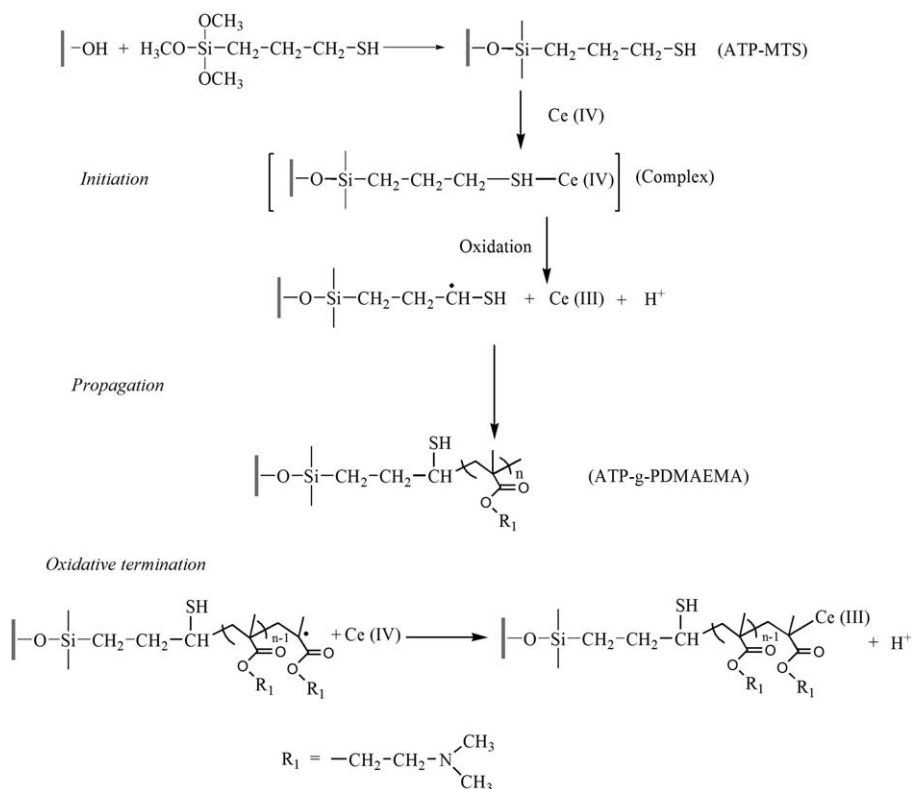
Scheme 1. Preparation of PDMAEMA grafted ATP via thiol-Ce (IV) initiated redox polymerization.

radicals initiated the polymerization of DMAEMA. Finally, ATP-g-PDMAEMA nanoparticles with core-shell structure were synthesized. Most importantly, surface free radicals were unique in this system, meaning the higher graft efficiency in comparison with the dual active sites redox initiation.

The surface chemical component and crystal structure of ATP and ATP-MTS are investigated using FTIR, XPS, and XRD. As shown in Figure 1(A), the FTIR spectrum of ATP shows a strong absorption band at 3550 cm^{-1} attributable to the stretching vibration of O—H. The absorption bands at 1038 and 988 cm^{-1} are attributed to the Si—O—Si framework bonds. After surface thiol functionalization, the anchoring propyl group on ATP-MTS is confirmed by the C—H stretching vibrations appeared at 2928 cm^{-1} and 2848 cm^{-1}, and bending vibration at 1452 and 1411 cm^{-1}. The weak but visible absorption band at 2565 cm^{-1} can be ascribed to the S—H stretching of MTS portion. Figure 1(B) shows that appreciable amounts of smectite, quartz, and calcite can be found in the XRD pattern of ATP except the main component phase. Three reflections at $2\theta = 8.43°$ (110), 13.68° (200), and 16.28° (130) were associated with the characteristic d spacing of ATP, respectively. The XRD analysis of ATP-MTS shows a small change in intensity of peaks but without any new peak. The XPS analysis of ATP suggests the presence of Si (103.3 eV, Si2p; 154.4 eV, Si2s), Mg (1304.4 eV, Mg1s), C (284.9 eV, C1s), and O (531.8 eV, O1s) elements in the wide-scan spectrum of ATP [Figure 1(C)]. The presence of thiol groups is verified by two peaks at 163.1 and 227.0 eV assigned to S2p and S2s, respectively, in the wide-scan spectrum of ATP-MTS. In addition, the C1s peak shows an obvious

increased intensity than ATP. The narrow scan C1s core-level spectrum of ATP-MTS can be curve-fitted with three peak components having Binding Energy (BE) at 283.7, 284.8, and 286.4 eV attributable to the C—Si, C—C/C—H, and C—S, respectively [Figure 1(D)].[41] All these experimental findings indicate the chemical anchoring of MTS on the surface of ATP-MTS particles.

The surface-initiated graft polymerization from the surface of ATP was carried out via a thiol-Ce (IV) redox initiation system to afford ATP-g-PDMAEMA hybrid particles. In the FTIR spectrum of ATP-g-PDMAEMA [Figure 2(A-i)], a typical peak at 1721 cm^{-1} attributed to C=O stretching vibration reveals the presence of grafted PDMAEMA. The peak at 1161 cm^{-1} is assigned to the C—N stretching vibration of PDMAEMA. It is noteworthy that a significant increase of the characteristic stretching bands of alkyl at 2994, 2925, 2854, and 1474 cm^{-1} can be observed while the spectrums of ATP-MTS and ATP-g-PDMAEMA are compared. Correspondingly, the FTIR of PDMAEMA obtained from homopolymerization in solution shows multiple bands in the range of 2700–2960 cm^{-1} corresponding to C—H stretching vibration of methyl and methylene. The peaks at 1450 cm^{-1} corresponding to the C—H bending, and the peak at 1720 cm^{-1} representing C=O stretching [Figure 2(A-ii)]. These FTIR results suggest that the grafting polymerization of DMAEMA from ATP surface was successfully realized. Furthermore, the XRD pattern of ATP-g-PDMAEMA shows that all main reflections have almost no changes in position except for weak changes in peak intensity [Figure 2(B)]. It can be possible to conclude that the crystal structure of ATP
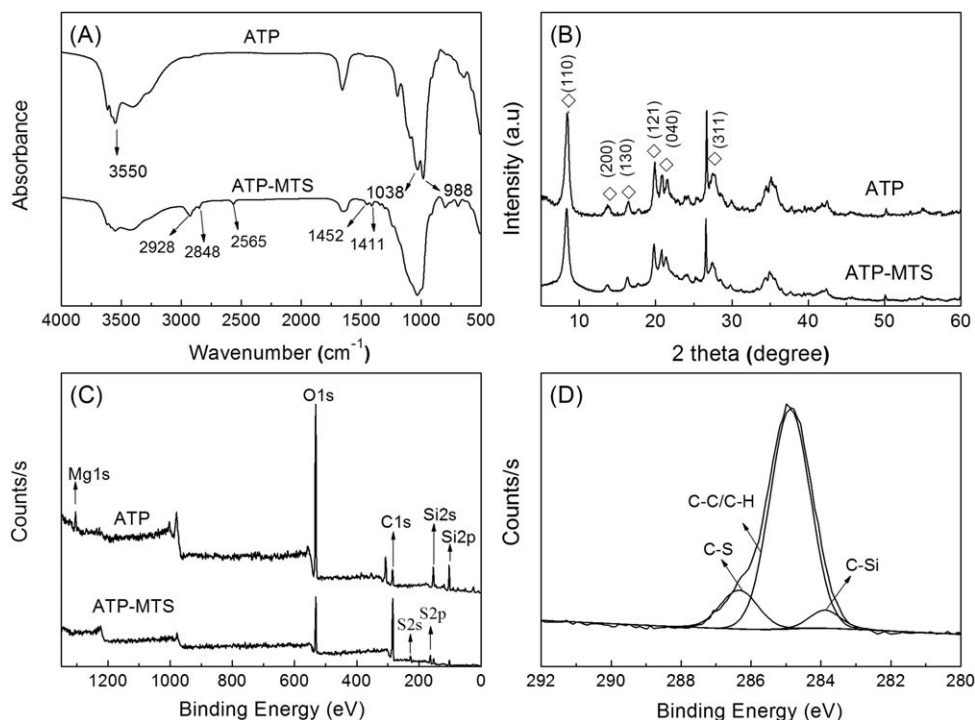
Figure 1. (A) FTIR spectrum, (B) XRD pattern, and (C) wide-scan spectrum of pristine ATP and ATP-MTS, and (D) C1s core-level spectrum of ATP-MTS.

was maintained during the graft polymerization process. As shown in the wide-scan spectrum of ATP-g-PDMAEMA, C1s peak presents a further enhancement compared with ATP-MTS,

and a new N1s peak at 400.1 eV can be observed [Figure 2(C)]. In the narrow scan of C1s core-level spectrum of ATP-g-PDMAEMA, the C1s peak resolves four peaks representing
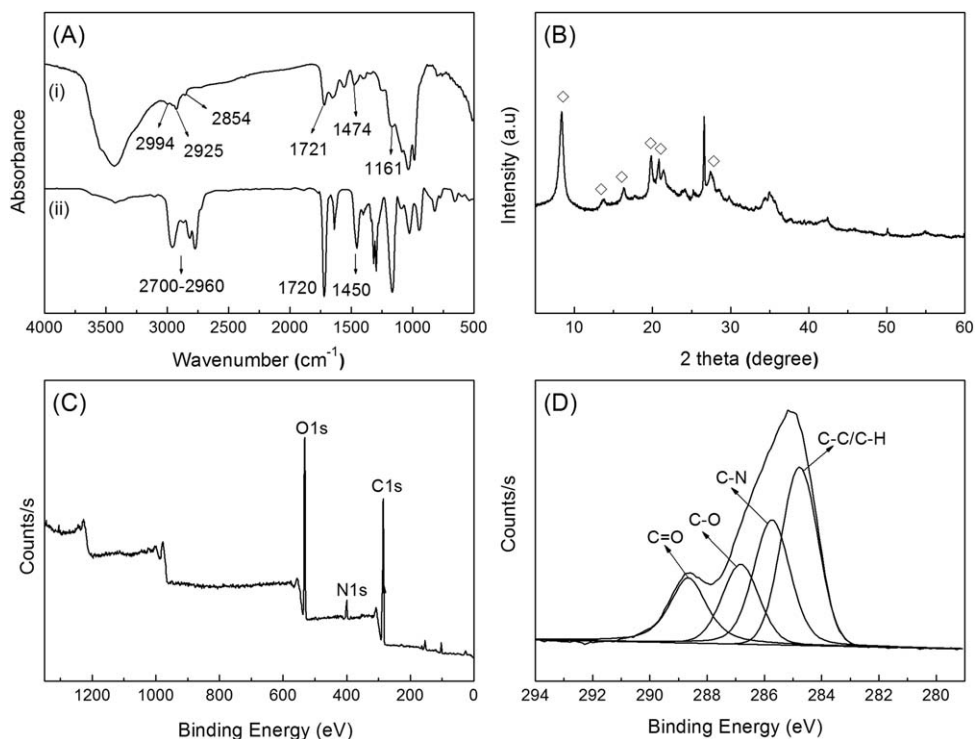

Figure 2. (A) FTIR spectrum of (i) ATP-g-PDMAEMA and (ii) pure PDMAEMA (from homopolymerization in solution), (B) XRD pattern, (C) wide-scan spectrum, and (D) C1s core-level spectrum of ATP-g-PDMAEMA.
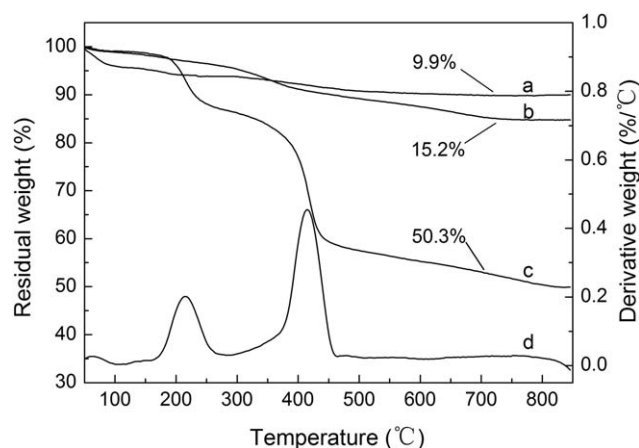
Figure 3. TGA curves and of (a) pristine ATP, (b) ATP-MTS, and (c) ATP-g-PDMAEMA after polymerization for 8 h; (d) DTG curve of ATP-g-PDMAEMA.

different carbons environment in PDMAEMA: aliphatic hydrocarbon (C—C/CH) at a BE of 284.8 eV, C—N of dimethylamino at 285.8 eV, C—O of ester at 286.8 eV, and the carboxyl carbon (C=O) at 288.7 eV [Figure 2(D)].[42]

TGA analyses of ATP, ATP-MTS, and ATP-g-PDMAEMA were undertaken at the temperature range from 50 to 850°C, and the results are shown in Figure 3. It is observed that the ATP loses 9.9% due to the weight loss of the absorbed water, zeolite water, crystal water, and structured water in ATP nanoparticles [Figure 3(a)]. After the surface modification, due to the decomposition of the organic composition on ATP surface, the weight loss of the grafted MTS on ATP is determined to be approximately 15.2% [Figure 3(b)]. As seen from Figure 3(d), the DTG curve of ATP-g-PDMAEMA nanocomposites shows two major decomposition peaks at 215 and 415°C corresponding to the side chains and backbone of PDMAEMA, respectively. The total weight loss of PDMAEMA grafted ATP is observed to attain to 50.3% after polymerization for 8 h [Figure 3(c)], and correspondingly PG is 35.1% calculated from eq. (1).

Variation of conversion, PG and GE with time is listed in Table I. It can be found that PG and GE increase with polymerization time, and the highest experimental value of GE is approximately 51.3% in comparison with 21.2% in the research we have reported previously.[39] Graft polymerization can contribute to the increase of PG substantially, even though the polymer grafting rate is smaller due to the relatively low concentration of the surface reactive sites. The decrease in GE may be attributed to the decrease in concentrations of initiator and the number of free radicals accessible for grafting as reaction proceeds. On the other hand, the kinetic barrier (inhibiting effect originated from already grafted chains) increases with the increase of conversion and PG. It is believed that the decrease in the rates of grafting reaction with increasing of PG results from the enforced diffusional resistance during grafting. Moreover, PDMAEMA is a kind of pH-sensitive polymer, and the pH of the system decreases as the graft polymerization. Grafted PDMAEMA chains are protonated and stretched with decreasing pH value, which results in a higher probability of bimolecular termination. These factors reduce the graft polymerization rate, followed by the decline of GE.

As seen in Scheme 1, Ce (IV) involves in the redox initiation and oxidative termination processes of graft polymerization synchronously. On the other hand, ceric ions in aqueous acidic solution consist of different species such as Ce (IV), Ce(OH) (III), and (Ce—O—Ce) (VII), and the component is depended on the acid concentration according to Scheme 2. As a whole, these reactions are influenced by the experimental temperature. Therefore, the reaction temperature, Ce (IV) and the acid concentration are taken into account in this study.

Firstly, by fixing the acid concentration and reaction temperature, the effect of the amount of Ce (IV) was studied to follow the impact on PG, and the results are presented in Figure 4. When Ce (IV) concentration is varied from 3.12×10^{-3} to 18.75×10^{-3} mol/L, PG increases with increasing Ce (IV) concentration up to 12.5×10^{-3} mol/L. This is attributed to the increase of initial radical sites on the surface of ATP-MTS. Above this level, a decreasing trend in PG is observed beyond 12.5×10^{-3} mol/L of Ce (IV) concentration. Excessive Ce (IV)
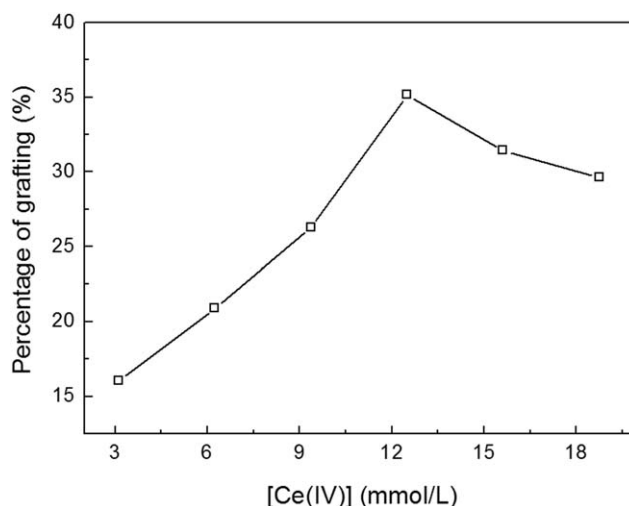
$$Ce(IV) + H_2O \rightleftharpoons (CeOH)(III) + H^+$$

$$2(CeOH)(III) \rightleftharpoons (Ce\text{-}O\text{-}Ce)(VI) + H_2O$$

Scheme 2. Hydrolysis reaction of Ce (IV) in an acidic environment.

Table I. Variation of Conversion, PG, and GE with Polymerization Time

Time (h)	Conversion (%)	PG (%)	GE (%)
0.5	1.4	2.9	43.8
1	2.7	6.1	45.7
2	6.7	13.9	47.9
4	15.2	27.5	49.9
5	18.0	31.6	51.3
6	20.7	33.3	48.2
8	22.7	35.1	47.5

Figure 4. Effect of Ce (IV) concentration on PG.

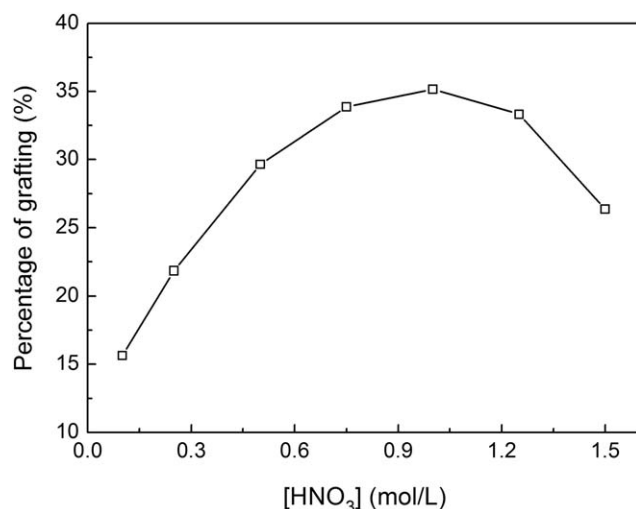**Figure 5.** Effect of HNO$_3$ concentration on PG.

Figure 6. Effect of polymerization temperature on PG.

also participates in the oxidative termination of graft polymerization, which reduces the surface radicals and decreases the polymerization rate. A great quantity of graft chains terminated prematurely at a lower degree of polymerization.

Subsequently, the effect of the acid concentration was investigated by varying the concentration from 0.1 to 1.5 mol/L. As shown in Figure 5, PG is found to initially increase up to the maximum when 1 mol/L of HNO$_3$ was used and then gradually decreased. According to Scheme 2, both of the equilibriums shift to the left when increasing the acid concentration, and therefore the higher acid concentration brings about higher Ce (IV) species and graft polymerization rate. On the other hand, protons are generated during redox initiation procedure as seen from Scheme 1. Consequently, the oxidation reaction of thiol-Ce (IV) complex is restrained significantly as an excessive HNO$_3$ concentration, which decelerates the initiation rate. What is more, the tertiary amine of PDMAEMA gets a proton to form quaternary ammonium in an acidic environment. PDMAEMA brushes are protonated and stretched along the radical direction due to the geometrical constraint, speeding up the bimolecular termination.[43]

The effect of temperature on PG was investigated over the 40–65°C range by keeping the other reaction condition constant. It can be seen from Figure 6 that PG increases with rise in tem-
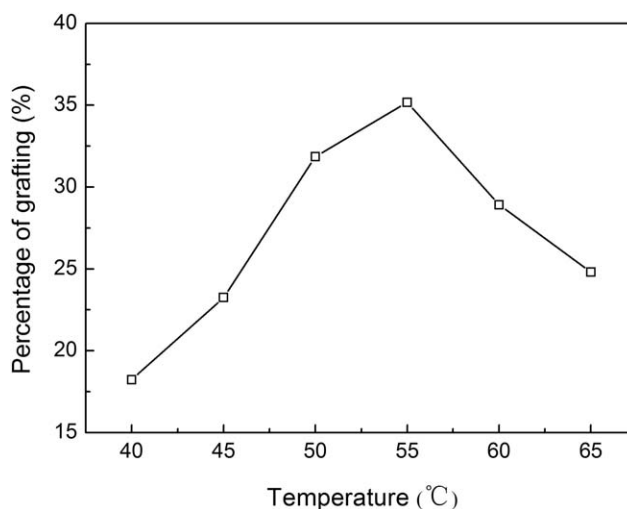
perature from 40 to 55°C, and decreases with further rise in temperature. The increase of PG with temperature can be ascribed to the acceleration of redox initiation and the diffusion of monomer. However, the positive effect of temperature is decreased due to the substantial increase in the rate of chain transfer and chain termination reactions when further increasing the reaction temperature. On the other hand, the kinetic barrier is formed prematurely at a higher temperature, which hinders the graft polymerization.

The TEM images of ATP and ATP-g-PDMAEMA are shown in Figure 7. It can be seen from Figure 7(A) that ATP exhibits a randomly oriented nano-scale fibril and relatively smooth surfaces with a diameter of 20–30 nm and several hundred of nanometers in length. As can be seen in Figure 7(B), ATP-g-PDMAEMA has similar fibers structure but a rough surface with an irregular diameter of 45–80 nm that is larger than that of ATP. This kind of morphology is agreement with the characteristic of surface-initiated conventional free radical polymerization.

CONCLUSIONS

In this work, a facile and effective preparation of PMDAEMA anchored on the surface of ATP by surface thiol-Ce (IV) initiated graft polymerization technique was demonstrated. ATP was
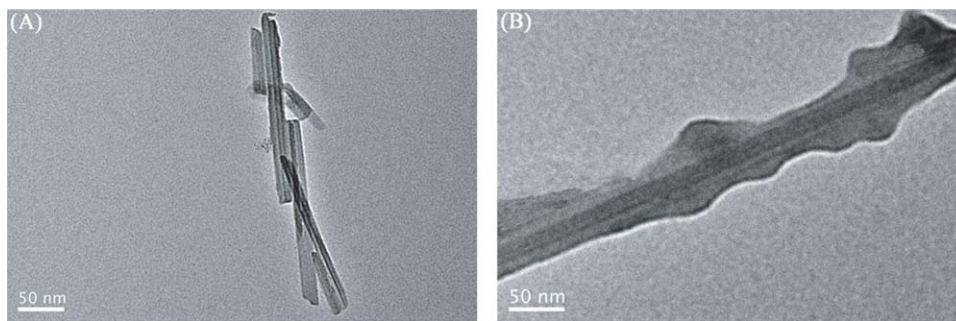

Figure 7. TEM images of (A) pristine ATP and (B) ATP-g-PDMAEMA hybrids. [Color figure can be viewed in the online issue, which is available at wileyonlinelibrary.com.]

functionalized by MTS to afford thiol-functionalized particles ATP-MTS. The surface-initiated graft polymerization of DMAEMA was carried out in HNO_3 aqueous solution in presence of ATP-MTS and CAN to synthesize ATP-g-PDMAEMA hybrids successfully. The study of FTIR, XPS, TGA, XRD, and TEM provided the evidence that graft polymerization was achieved successfully. It was observed that surface grafting by PDMAEMA had no effect on the crystal structure of ATP suggested by XRD analysis. For the surface-initiated polymerization under the optimal condition, PG of grafting PDMAEMA reached to 35.1% after 8 h of polymerization according to TGA results.

ACKNOWLEDGMENTS

REFERENCES

1. Golden, J. H.; Deng, H. B.; Disalvo, F. J.; Thompson, P. M.; Frechet, J. M. Science 1995, 268, 1463.

2. Kickelbick, G. Prog. Polym. Sci. 2003, 28, 83.

3. Kim, J. Y.; Koo, H. M.; Ihn, K. J.; Suh, K. D. J. Ind. Eng. Chem. 2009, 15, 103.

4. Liu, C. H.; Pan, C. Y. Polymer 2007, 48, 3679.

5. Kango, S.; Kalia, S.; Celli, A.; Njuguna, J.; Habibi, Y.; Kumar, R. Prog. Polym. Sci. 2013, 38, 1232.

6. Zdyko, B.; Luzinov, I. Macromol. Rapid Commun. 2011, 32, 859.

7. Bach, L. G.; Islam, M. R.; Kim, J. T.; Seo, S. Y.; Lim, K. T. Appl. Surf. Sci. 2012, 258, 2959.

8. Radhakrishnan, B.; Ranjan, R.; Brittain, W. J. Soft Matter 2006, 2, 386.

9. Dong, H. C.; Huang, J. Y.; Koepsel, R. R.; Ye, P. L.; Russell, A. J.; Matyjaszewski, K. Biomacromolecules 2011, 12, 1305.

10. Hwang, H. S.; Bae, J. H.; Kim, H. G.; Lim, K. T. Eur. Polym. J. 2010, 46, 1654.

11. Landfester, K.; Rothe, R.; Antonietti, M. Macromolecules 2002, 35, 1658.

12. Cai, R.; Deng, B.; Jiang, H. Q.; Yu, Y.; Yu, M.; Li, L. F.; Li, J. Y. Radiat. Phys. Chem. 2012, 81, 1354.

13. Yang, D. S.; Jung, D. J.; Choi, S. H. Radiat. Phys. Chem. 2010, 79, 434.

14. Monteiro, M. J.; Cunningham, M. F. Macromolecules 2012, 45, 4939.

15. Pokorski, J. K.; Breitenkamp, K.; Liepold, L. O.; Qazi, S.; Finn, M. G. J. Am. Chem. Soc. 2011, 133, 9242.

16. Rodriguez-Emmenegger, C.; Hasan, E.; Pop-Georgievski, O.; Houska, M.; Brynda, E.; Alles, A. B. Macromol. Biosci. 2012, 12, 525.

17. Tsubokawa, N.; Kogure, A.; Maruyama, K.; Sone, Y.; Shimomura, M. Polym. J. 1990, 22, 827.

18. Tsubokawa, N.; Ishida, H. J. Polym. Sci. Part A: Polym. Chem. 1992, 30, 2241.

19. Hayashi, S.; Takeuchi, Y.; Eguchi, M.; Lida, T.; Tsubokawa, N. J. Appl. Polym. Sci. 1999, 71, 1491.

20. Sarac, A. S. Prog. Polym. Sci. 1999, 24, 1149.

21. Wang, Y. P.; Yuan, K. Y.; Li, Q. L.; Wang, L. P.; Gu, S. J.; Pei, X. W. Mater. Lett. 2005, 59, 1736.

22. Zhang, Y. Y.; Gao, B. J.; Gu, L. Y.; Zhao, X. L. Acta Polym. Sin. (in Chinese) 2012, 56, 264.

23. Yao, R. R.; Wu, R.; Zhai, G. Q. Polym. Eng. Sci. 2015, 55, 735.

24. Nair, V.; Deepthi, A. Chem. Rev. 2007, 107, 1862.

25. Nair, V.; Balagopal, L.; Rajan, R.; Mathew, J. Acc. Chem. Res. 2004, 37, 21.

26. Yagci, C.; Yildiz, U. Eur. Polym. J. 2005, 41, 177.

27. Joshi, J. M.; Sinha, V. K. Carbohydr. Polym. 2007, 67, 427.

28. Samal, R. K.; Nayak, M. C.; Panda, G.; Suryanarayana, G. V.; Das, D. P. J. Polym. Sci. Part A: Polym. Chem. 1982, 20, 53.

29. Erbil, C.; Cin, C.; Soydan, A. B.; Sarac, A. S. J. Appl. Polym. Sci. 1993, 47, 1643.

30. Shimomura, M.; Kikuchi, H.; Yamauchi, T.; Miyauchi, S. J. Macromol. Sci. Part A: Pure. Appl. Chem. 1996, 33, 1687.

31. Jiang, L.; Huang, W. Y.; Xue, X. Q.; Yang, H. J.; Jiang, B. B.; Zhang, D. L.; Fang, J. B.; Chen, J. H.; Yang, Y.; Zhai, G. Q.; Kong, L. Z.; Wang, S. F. Macromolecules 2012, 45, 4092.

32. O'Brien, J. L.; Gornick, F. J. Am. Chem. Soc. 1955, 77, 4757.

33. Bradley, W. F. Am. Mineral. 1940, 25, 405.

34. Neaman, A.; Singer, A. Appl. Clay. Sci. 2004, 25, 121.

35. Huang, J. J.; Liu, Y. F.; Jin, Q. Z.; Wang, X. G.; Yang, J. J. Hazard. Mater. 2007, 143, 541.

36. Li, X.; Zong, Z. M.; Ma, W. W.; Cao, J. P.; Mayyas, M.; Wei, Z. H.; Li, Yan.; Yan, H. L.; Wang, D.; Yang, R.; Wei, X. D. Fuel. Process. Technol. 2015, 134, 39.

37. Yang, H. C.; Zhang, L.; Ma, W. Z.; Pu, H. T.; Gong, F. H. J. Appl. Polym. Sci. 2015, 132, 3031.

38. Yang, H. C.; Pu, H. T.; Gong, F. H. J. Appl. Polym. Sci. 2014, 131, 11730.

39. Zhang, L.; Yang, H. C.; Liu, H.; Ni, Q. T.; Gong, F. H. Polym. Eng. Sci. 2015, 55, 889.

40. Xu, H.; Yang, H. C.; Zhang, L.; Chen, Y.; Ni, Q. T.; Gong, F. H. Acta Polym. Sin. (in Chinese) 2015, 59, 437.

41. Vogt, A. D.; Han, T.; Beebe, T. P. Langmuir 1997, 13, 3397.

42. Wang, W. P.; Tang, J. Y.; Jia, Z. Q.; Li, X. X.; Xiao, Z. H. J. Polym. Res. 2012, 19, 9804.

43. Zhou, L. L.; Yuan, W. Z.; Yuan, J. Y.; Hong, X. Y. Mater. Lett. 2008, 62, 1372.